# PVP-functionalized nanometre scale metal oxide coatings for cathode materials: successful application to $LiMn_2O_4$ spinel nanoparticles†

**Sunhye Lim and Jaephil Cho**

*Received (in Cambridge, UK) 9th May 2008, Accepted 11th June 2008*
*First published as an Advance Article on the web 30th July 2008*
**DOI: 10.1039/b807973k**

**PVP functionalized metal oxide coatings on spinel nanoparticles demonstrated significantly improved rate characteristics under extensive cycling at 65 °C and exhibited over 100% improved capacity retention compared to the bare counterpart.**

Spinel $LiMn_2O_4$ cathodes have been studied for possible use in Li-ion cells for hybrid electric vehicles (HEVs). However, the delithiated product $Li_0Mn_2O_4$, referred to as λ-$MnO_2$, may react with the electrolyte, leading to passivating structural changes of the active material at elevated temperatures.[1–3] Substantial research has indicated that the capacity fade of 4 V $Li/Li_xMn_2O_4$ cells can be largely attributed to the solubility effects at the spinel-electrode surface and that the soluble ion is a $Mn^{2+}$-ion containing species. However, such changes seem to occur to a lesser extent when using $Li_{1+x}Mn_{2-x}O_4$ type spinels cycling at temperatures less than 55 °C, which have reduced capacity fade, but lower initial capacity.[4,5]

In order to minimize the Mn solubility that governs the catalytic activity of $LiMn_2O_4$ specimens, the surface reactivity of the spinel with electrolytes is the most important parameter to ensure cycling stability above 50 °C.[6,7] Therefore, surface coating has been regarded as the most promising solution for minimizing Mn dissolution, and solution-based techniques, such as sol–gel, solution precipitation, and the sonochemical method, have been used for improving the high temperature cycling of the spinels.[8–18] However, these methods cannot lead to a uniform coating layer and can lead to difficulty in controlling the coating thickness as the coating precursors randomly adhere to the active materials during drying and annealing. Hence, coating with a uniform thickness is very difficult to control, and the segregation of the coating is inevitable. If a metal oxide is uniformly coated on the spinels, capacity fade from the Mn dissolution should be significantly reduced, especially under extended cycling above 60 °C, which is a critical temperature for HEV application. In addition, it is very challenging to produce a uniform coating on nanoparticles compared to coating on bulk particles. Recently, spinels prepared by tailoring the morphology (mesoporous and hollow)[19–21] or atomic layer deposition[22] have been studied to improve the rate capabilities at room temperature.[19–21] However, no studies for improving both the rate capability and cycle life performance above 60 °C have been reported.

In this study, a new metal oxide coating method that leads to a uniform coating layer and control of coating thickness *via* functionalized spinel surfaces with polyvinyl pyrrolidone (PVP) is reported. This new coating method was successfully applied to spinel nanoparticles with a high surface area. Furthermore, MgO and $Al_2O_3$ coatings resulted in superior capacity retention at 65 °C cycling compared to uncoated and coated spinels without PVP.

Fig. 1a shows a schematic diagram for the PVP-functionalized metal oxide coating procedure, and as-synthesized spinel nanoparticles were functionalized with PVP groups in distilled water. Dissolved metal ions were then complexed with the entire PVP backbone, and the remaining ionic groups ($NO_3^-$ or $C_2O_4^-$) dissolved in water were removed by filtering. The filtered powder was heat-treated at 600 °C for 3 h in air. However, the previous coatings used a mixed slurry containing the coating solution and cathode powder for drying and the annealing processes. Accordingly, it was impossible to produce a uniform coating layer. Fig. 1b shows an SEM image of the uncoated spinel nanoparticles with a size smaller than 90 nm. Fig. 1c indicates that the surface morphology of the PVP-functionalized spinel nanoparticles with absorbed $Mg^{2+}$ ions after drying at 100 °C is completely different from that of the uncoated spinel nanoparticles.

Element mapping of Mg atoms using energy dispersive X-ray spectroscopy (EDXS) confirms the presence of Mg throughout the particles (inset of c). After annealing at 600 °C for 3 h, the surface morphology is similar to that of the uncoated spinels

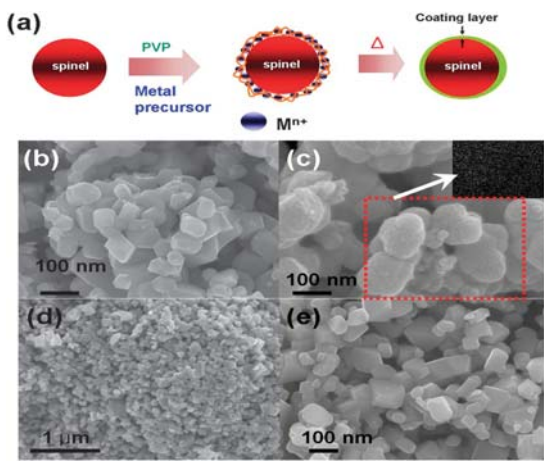


**Fig. 1** (a) Schematic diagram of the metal oxide coating procedure and SEM images of (b) uncoated spinel nanoparticles, (c) MgO-coated PVP-functionalized spinel nanoparticles after drying at 100 °C (inset of (c) is EDXS of Mg in the particles within the red line), and (d) and (e) SEM images of (c) after annealing at 600 °C for 3 h in air.

*Department of Applied Chemistry, Hanyang University, Sa-Dong, Ansan, Korea 426-791. E-mail: jpcho@hanyang.ac.kr; Tel: +82314005508*

† Electronic supplementary information (ESI) available: A typical experimental procedure for the uncoated and coated spinel nanoparticles and characterization methods, TEM images of the coated nanoparticles without using PVP, XRD patterns of the cycled electrodes. See DOI: 10.1039/b807973k

 

(the same morphology change after $Al_2O_3$ coating). XRD patterns of the bare, 1 wt% MgO or $Al_2O_3$-coated spinels were indexed based on the cubic spinel structure with a space group of $Fd\bar{3}m$. The lattice constant $a$ of the uncoated and coated spinels was estimated to be 8.238 ± 0.005 Å and 8.236 ± 0.005 Å, respectively (ESI Fig. S1†). 1 wt% Metal-coated spinels refer to 1 wt% metal oxide-coated spinel nanoparticles obtained from the thermal annealing of the functionalized PVP with absorbed metal ions at 600 °C in air (amount of metal precursor relative to that of the spinel powder was 3 wt%).

Shown in Fig. 2a and c, are the cross-sectional TEM images of the PVP-functionalized $Al_2O_3$ and MgO-coated spinel particles after annealing at 600 °C. The ramp rate used for reaching 600 °C was 3 °C $min^{-1}$ and the particles were maintained at this temperature for 3 h. When the fast ramp rate was used, the coating thickness was irregular. This result indicates that a slow burn-out of PVP is necessary to have a uniform coating layer. The images show uniform coating layers with a thickness of ~8 nm, and the $Al_2O_3$-coated sample had a rough surface morphology, compared to the MgO-coated nanoparticles after annealing at 600 °C. The inset of image a is the HREM image of the $Al_2O_3$ coating layer (dotted circle), and no lattice fringes are observed, which indicates the formation of an amorphous phase. The line scan (image b) of an $Al_2O_3$-coated nanoparticle across the red line on image a shows co-diffused Al and Mn atoms in the bulk and coating layer, indicating the formation of an amorphous Li–Mn–Al–O solid solution. This solid solution is believed to provide the Li-ion conduction pathways. The same phenomenon in MgO-coated spinel nanoparticles, as shown in Fig. 2c, d, and e, is observed, although the coating layer seems to be denser than for the $Al_2O_3$-coated nanoparticles. The specific surface area determined by Brunauer–Emmet–Teller (BET) measurements of the uncoated sample was 19 $m^2 g^{-1}$, and was 19 and 18 $m^2 g^{-1}$ for the 1 wt% $Al_2O_3$ or MgO-coated spinels.

When the spinel nanoparticles were coated with the same concentration of $Mg_2C_2O_4$ or Al nitrate precursors without PVP, the coating thickness was not uniform and approximately varied from 5 to 20 nm (ESI Fig. S2†). It has been reported that PVP can trap $M^{n+}$ ions.[23,24] $Mg^{2+}$ ions can bind to the PVP-capped spinel particles, and depending on the amount PVP of used, the coating thickness can be controlled. When the amounts of PVP and metal oxide precursors were increased by a factor of two, the coating thickness increased to 20 nm (ESI Fig. S3†). However, when the amount of only the metal oxide precursors was doubled, the coating thickness was not increased effectively. This means that all of these metal ions were not complexed with the entire PVP backbone.

Fig. 3 shows the first cycling curves of the bare and 1 wt% MgO coated spinels under 0.2, 1, 3, 5, and 7 C (1 C = 140 mA $g^{-1}$) rates at 65 °C. The uncoated cathode shows first charge and discharge capacities of 138 and 129 mAh $g^{-1}$, respectively, with a Coulombic efficiency of 93%. The discharge capacities at rates of 1, 3, 5, and 7 C are 117, 114, 105, and 78 mAh $g^{-1}$, respectively, with a capacity retention of 66% at a rate compared to 1 C. Alternatively, the 1 wt% MgO-coated spinel nanoparticles show first charge and

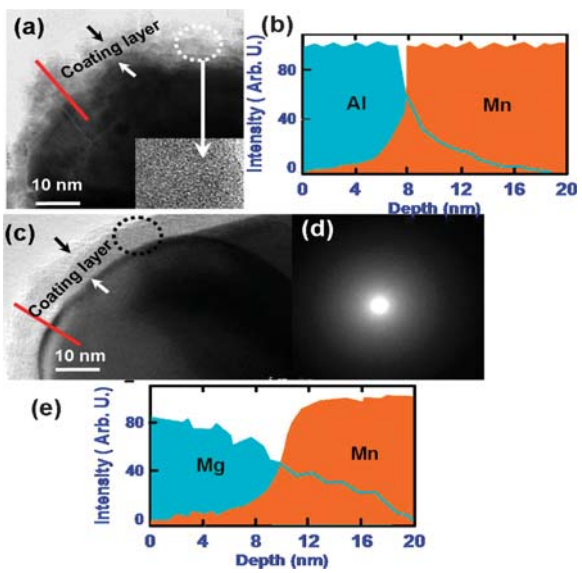


**Fig. 2** (a) TEM images of a cross-section of an $Al_2O_3$-coated spinel nanoparticle after annealing the functionalized spinel nanoparticles at 600 °C (inset is an HREM image of the coating layer indicated with the dotted white circle); (b) line scan of Al and Mn along the red line in image a; (c) TEM images of a cross-section of a MgO-coated spinel nanoparticle after annealing the functionalized spinel nanoparticles at 600 °C; (d) selected area diffraction patterns of the coating layer indicated with the dotted black circle; and (e) line scan of Mg and Mn along the red line in image c.

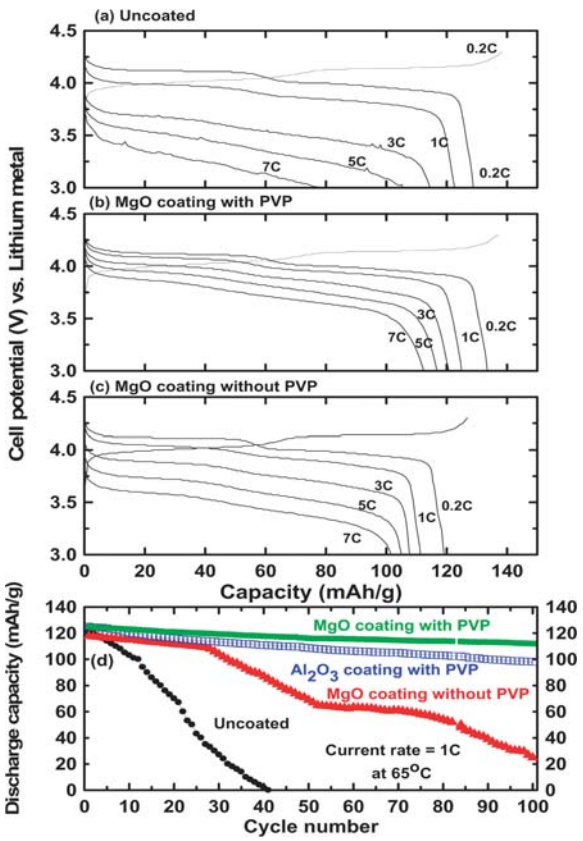


**Fig. 3** (a), (b), and (c) Respective first cycling curves of the bare and 1 wt% MgO-coated spinels with and without PVP functionalization under 0.2, 1, 3, 5, and 7 C (1 C = 140 mA $g^{-1}$) rates at 65 °C (the cells were cycled once at different C rates), and (d) plot of discharge capacity as a function of the cycle number of the bare, and 1 wt% MgO and $Al_2O_3$-coated spinels functionalized with PVP out to 95 cycles at a rate of 1 C in coin-type half cells between 3 and 4.3 V at 65 °C.

discharge capacity values of 137 mAh $g^{-1}$ and 134 mAh $g^{-1}$, respectively, with a Coulombic efficiency of 98% and a 5% improvement compared to the uncoated sample. The discharge capacities at rates of 1, 3, 5, and 7 C (1 C = 140 mA $g^{-1}$) are 129, 125, 121, and 119 mAh $g^{-1}$. The capacity retention at a 7 C rate is 92%, an improvement of 26% from the bare cathode. Alternatively, 1 wt% MgO-coated spinels without functionalizing PVP show a decrease of discharge capacity to 119 mAh $g^{-1}$, and with increasing C rates, the initial voltage drop is greater than that for the same material with functionalizing PVP. This indicates the enhanced structural degradation of the spinel particles. For example, the first discharge voltages of the MgO-coated spinels with and without functionalizing PVP were 4.1 V and 3.8 V, respectively. The discharge capacity of the MgO-coated spinels without functionalizing PVP is 102 mAh $g^{-1}$ at a rate of 7 C, which is less than with functionalizing PVP. Moreover, when the cycling test is performed at a 1 C rate for 95 cycles at 65 °C, the capacity retention difference was more significant. Fig. 3d shows the cycle life performance of the uncoated, 1 wt% $Al_2O_3$, and MgO-coated spinels functionalized with or without PVP at 65 °C for 90 cycles at a rate of 1 C between 3 and 4.3 V in coin-type half cells. The capacity retention of the uncoated sample approaches zero after 35 cycles, while MgO and $Al_2O_3$-coated samples show 95% and 90% retention, respectively. The improved capacity retention of the cell containing the MgO coating compared to the $Al_2O_3$ coating is believed to be due to the denser coating. However, the MgO-coated sample without functionalizing PVP shows a capacity fade similar to that with functionalizing PVP up to 30 cycles, after which a rapid fade out to 100 cycles is observed with a capacity retention of 10%. This is due to localized coating and an abnormally thick coating layer (ESI Fig. S2†).

Compared with previous studies using metal oxide coatings, the results show much improved results even though the cells were tested at a higher temperature. In the case of 5.5 wt% MgO-coated $LiMn_2O_4$ prepared by the sonochemical method,[13] a discharge capacity of ~65 mAh $g^{-1}$ from a first discharge capacity of 118 mAh $g^{-1}$ was shown, while an uncoated bulk sample decreased from 50 mAh $g^{-1}$ to 120 mAh $g^{-1}$ after 100 cycles at 60 °C and a rate of 0.2 C. In the case of 3–5 wt% $Al_2O_3$-coated $LiMn_2O_4$ prepared by a solution method,[11] the discharge capacity after 100 cycles was 109 mAh $g^{-1}$ from a first discharge capacity of 130 mAh $g^{-1}$ at 60 °C and a rate of 0.5 C. However, an uncoated sample delivered over 60% capacity retention, showing a discharge capacity of 78 mAh $g^{-1}$ from a first discharge capacity of 132 mAh $g^{-1}$, even after 100 cycles at 60 °C. Much improved capacity retention of the uncoated sample in this study, compared to our uncoated sample is due to the difference in BET surface area, and previous research used commercially available spinel powder, which usually has a BET surface area $<2$ $m^2$ $g^{-1}$. It has been reported that capacity loss at 55 °C is increased by a factor of two when the BET surface area increases by a factor of six.[7]

The amount of dissolved Mn significantly increases in the uncoated cathode after 100 cycles, to 8000 ppm, but it decreases to 130 ppm for the coated cathode functionalized with PVP (the amount of the dissolved Mn in all the samples before cycling was negligible, showing $<40$ ppm). Alternatively, the amount in the coated cathode without functionalizing PVP was 6000 ppm, demonstrating that Mn dissolution was the main source of poor cycling performance at 65 °C, and the substantial amount of Mn dissolution indicates that dissolution was an integral part of the overall elevated temperature failure mechanism. XRD diffraction data of the cycled electrode also show more defective phase formation in the uncoated and MgO coating without PVP functionalization than in MgO coating with PVP functionalization (ESI Fig. S4†). In this regard, uniform MgO and $Al_2O_3$ coatings throughout the PVP are very effective in reducing the reactivity at the spinel surface and electrolyte interface.

In conclusion, PVP functionalized metal oxide coatings on spinel nanoparticles demonstrated significantly improved rate characteristics under extensive cycling at 65 °C and exhibited over 100% improved capacity retention compared to the bare counterpart. The improved rate and capacity retention were associated with the uniform and dense MgO coating layer minimizing the Mn dissolution from the spinel lattice. It is believed that this simple new coating method can be used on other cathode materials, such as $LiCoO_2$, $LiFePO_4$, and $LiNi_{1-x}M_xO_2$.

This work was supported by the IT R&D program of MIC/IITA (2006-S-057-01, 4.35 V Cathode Material for Cellular Phone Power Source).

## Notes and references


1 M. M. Thackeray, *Prog. Solid State Chem.*, 1997, **25**, 1.
2 A. Blyr, C. Sigala, G. G. Amatucci, D. Guyomard, Y. Chabre and J. M. Tarascon, *J. Electrochem. Soc.*, 1998, **145**, 194.
3 R. J. Gummow, A. de Kock and M. M. Thackeray, *Solid State Ionics*, 1994, **69**, 59.
4 Y. Xia and M. Yoshio, in *Lithium Batteries Science and Technology*, ed. G.-A. Nazri and G.-A. Pistoia, Kluwer, Boston, 2004, p. 361.
5 M. Wakihara, G. Li and H. Ikuta, in *Lithium Batteries—Fundamentals and Performance*, ed. M. Wakihara and O. Yamamoto, Kodansha, Japan and Wiley-VCH, Germany, 1998, p. 26.
6 M. Yoshio, Y. Xia, N. Kumada and S. Ma, *J. Power Sources*, 2001, **101**, 79.
7 G. G. Amatucci, C. N. Schmutz, A. Blyr, C. Sigala, A. S. Gozdz, D. Larcher and J. M. Tarascon, *J. Power Sources*, 1996, **69**, 11.
8 Z. Liu, H. Wang, L. Fang, J. Y. Lee and L. M. Gan, *J. Power Sources*, 2002, **104**, 101.
9 H. Kweon, G. Kim and D. Park, US Pat. 6,183,911, 2001.
10 Z. Zheng, Z. Tang, Z. Zhang, W. Shen and Y. Lin, *Solid State Ionics*, 2002, **148**, 317.
11 A. M. Kannan and A. Manthiram, *Electrochem. Solid-State Lett.*, 2002, **5**, A167.
12 J. Cho, G. B. Kim, H. S. Lim, C. Kim and S. Yoo, *Electrochem. Solid-State Lett.*, 1999, **2**, 607.
13 J. S. Gnanaraj, V. G. Pol, A. Gedanken and D. Aurbach, *Electrochem. Commun.*, 2003, **5**, 940.
14 G. G. Amatucci, A. Blyr, C. Siagala, P. Alfonse and J. M. Tarascon, *Solid State Ionics*, 1997, **104**, 222.
15 J. Cho, Y. Kim and Y. Kim, *Chem. Commun.*, 2001, 1074.
16 J.-M. Han, S.-T. Myung and Y.-K. Sun, *J. Electrochem. Soc.*, 2006, **153**, A1290.
17 J. Cho, Y. J. Kim, T.-J. Kim and B. Park, *Angew. Chem., Int. Ed.*, 2001, **40**, 3367.
18 J. Cho, Y.-W. Kim, B. Kim, J.-G. Lee and B. Park, *Angew. Chem., Int. Ed.*, 2003, **42**, 1618.
19 J.-Y. Luo, Y.-G. Wang, H.-M. Xiong and Y. Xia, *Chem. Mater.*, 2007, **19**, 4791.
20 J.-Y. Luo and Y. Xia, *Adv. Funct. Mater.*, 2007, **17**, 3877.
21 J. Y. Luo, L. Cheng and Y. Y. Xia, *Electrochem. Commun.*, 2007, **9**, 1404.
22 M. Q. Snyder, S. A. Trebukhova, B. Ravdel, M. C. Wheeler, J. DiCarlo, C. P. Tripp and W. J. DeSisto, *J. Power Sources*, 2007, **165**, 379.
23 H. A. Maturana, I. M. Peric, S. A. Pooley and B. L. Rivas, *Polym. Bull.*, 2000, **45**, 425.
24 M. W. Pitcher, Y. He and P. A. Bianconi, *Mater. Chem. Phys.*, 2005, **90**, 57.


 